

A Proposed PAPR and BER Reduction Method For 4G-LTE-SCFDMA Using The Multiwavelet Transform

RAAD FARHOOD CHISAB

AKTHAM HASAN ALI

SALAM KHALAF ABDULLAH

Institute of Technology-Baghdad

Foundation of Technical Education

IRAQ

PROF. DR. C. K. SHUKLA

Professor

Dept. of ECE SHIATS (Deemed to be University)

Allahabad, UP

INDIA

Abstract

Single Carrier Frequency Division Multiple Access (SCFDMA) has been endorsed in the Long Term Evolution (LTE) standard for the uplink technique. It is enticing much advantage due to its capability to give lower bit error rate (BER) and peak to average power ratio (PAPR) as compared with the downlink system in LTE. In this paper an improved SCFDMA is proposed which built on the Multiwavelet Transform (MWT) instead of the Fast Fourier Transform (FFT). The results demonstrate that the new modified SCFDMA gives lower BER and decrease the PAPR in all cases when change parameters such as roll off factor, subcarrier mapping and modulation type under the LTE channel model.

Keywords: LTE, MWT, SCFDMA, BER, PAPR

Introduction

In order to make all the consumers share system resources in broad-band wireless communication, the researcher designed miscellaneous multiple access classes, as shown in Fig. 1. OFDM makes total sub-carriers orthogonal and overlapping. Because of its more PAPR comparing with the single-carrier system, OFDM can raise the cost of power amplifier and is not worthy for uplink implementation. SC-FDMA is a novel kind of FDMA system which was proposed in recent years. It has the analogous PAPR as single-carrier scheme and its resource scheduling is as supple as multi-carrier system. So it can be used for uplink application in broad-band wireless communication such as LTE [1].

SC-FDMA has a knowingly lesser PAPR compared to downlink technique. This considerably improves its RF power amplifier competence and also the mean power output from a battery driven mobile user [2]. High PAPR is mostly unsafe for uplink mobile equipment, given the power bounds at the mobile user. Little PAPR of the SCFDMA sending signal marks it as a very smart solution for the mobile uplink [3].

In this paper a new method for reduction BER and PAPR is proposed which depends on change the main transform in the system which is the FFT and replace it with the MWT. Note that all the tests of BER will be done under the LTE channel model which is invented by 3GPP. This paper is organized as: in the beginning give brief information about the SCFDMA and its specification then give minor information about the Multiwavelet transform. Then a modified system is described in details finally show the simulation results and graph for BER and PAPR. Finally, gives brief conclusion.

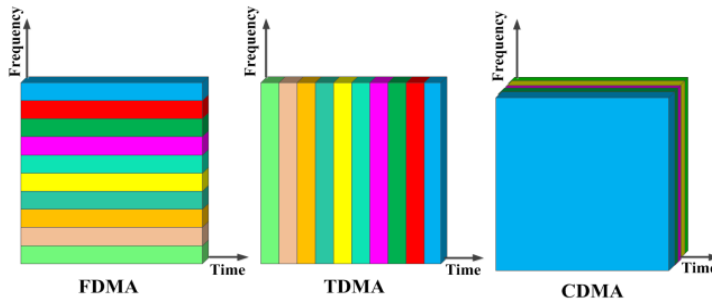


Figure 1: Examples of multiple access approaches

MULTI WAVELET TRANSFORM

Multiwavelet Transform was presented previously and found wide spread application in several fields due to the orthogonality of basis functions and their enhanced fitness for use in signal processing [4]. Multiwavelet has skills to drop the inter symbol interference and inter carrier interference, which are created by the damage in orthogonality between the carriers [5]. Multiwavelet gives immediate orthogonal property, symmetrical, and short support which do not exist and impossible with scalar two-channel wavelet structures [6]. The augmentations of Multiwavelet and their encouraging features in applications have engrossed a great agreement of interest and effort in latest years [7].

For notational suitability, the set of scaling function $\Phi(t)$ and Multiwavelet function $\Psi(t)$ can be written by using the symbolization [8].

$$[\Phi(t)] = [\Phi_1(t) \ \Phi_2(t) \ \dots \ \Phi_r(t)]^T \quad (1)$$

$$[\Psi(t)] = [\Psi_1(t) \ \Psi_2(t) \ \dots \ \Psi_r(t)]^T \tag{2}$$

The Multiwavelet regards till now for $r=2$. The GHM two scaling and wavelet function satisfy the next two scale dilation equations [9].

$$\begin{bmatrix} \Phi_1(t) \\ \Phi_2(t) \end{bmatrix} = \sqrt{2} \sum_k H_k \begin{bmatrix} \Phi_1(2t-k) \\ \Phi_2(2t-k) \end{bmatrix} \tag{3}$$

$$\begin{bmatrix} \Psi_1(t) \\ \Psi_2(t) \end{bmatrix} = \sqrt{2} \sum_k G_k \begin{bmatrix} \Psi_1(2t-k) \\ \Psi_2(2t-k) \end{bmatrix} \tag{4}$$

Then $H(k)$ and $G(k)$ are formed as a matrix filter such as [10]:

$$[H_k] = \begin{bmatrix} h_0(2k) & h_0(2k+1) \\ h_1(2k) & h_1(2k+1) \end{bmatrix} \tag{5}$$

$$[G_k] = \begin{bmatrix} g_0(2k) & g_0(2k+1) \\ g_1(2k) & g_1(2k+1) \end{bmatrix} \tag{6}$$

$$\sum_k h_0(k)^2 = 1 \ , \ \sum_k h_1(k)^2 = 1 \tag{7}$$

$$\sum_k g_0(k)^2 = 1 \ , \ \sum_k g_1(k)^2 = 1 \tag{8}$$

Therefore the matrix filters $H(k)$ and $G(k)$ can be describes and formed as [11]:

$$[H_0] = \frac{1}{20\sqrt{2}} \begin{bmatrix} 12 & 16\sqrt{2} \\ -\sqrt{2} & -6 \end{bmatrix}, \quad [H_1] = \frac{1}{20\sqrt{2}} \begin{bmatrix} 12 & 0 \\ 9\sqrt{2} & 20 \end{bmatrix} \tag{9}$$

$$[H_2] = \frac{1}{20\sqrt{2}} \begin{bmatrix} 0 & 0 \\ 9\sqrt{2} & -6 \end{bmatrix}, \quad [H_3] = \frac{1}{20\sqrt{2}} \begin{bmatrix} 0 & 0 \\ -\sqrt{2} & 0 \end{bmatrix} \tag{10}$$

$$[G_0] = \frac{1}{20\sqrt{2}} \begin{bmatrix} -\sqrt{2} & -6 \\ 2 & 6\sqrt{2} \end{bmatrix}, \quad [G_1] = \frac{1}{20\sqrt{2}} \begin{bmatrix} 9\sqrt{2} & -20 \\ -18 & 0 \end{bmatrix} \tag{11}$$

$$[G_2] = \frac{1}{20\sqrt{2}} \begin{bmatrix} 9\sqrt{2} & -6 \\ 18 & -6\sqrt{2} \end{bmatrix}, \quad [G_3] = \frac{1}{20\sqrt{2}} \begin{bmatrix} -\sqrt{2} & 0 \\ -2 & 0 \end{bmatrix} \tag{12}$$

PROPOSED SCHEME OF 4G-LTE-SCFDMA

In MWT-LTE-SC-FDMA system as in Fig. 2, the data input block is $[d_k] = [d_0 \ d_1 \ d_2 \ \dots \ d_K]$. $K \gg N$, N is the no. of carrier. First, the data $[d]$ enters to the first block which is the QPSK modulation block. The signal can be written as:

$$sa(t) = \sqrt{\frac{2E_s}{T_s}} \cos\left(2\pi f_c t + (2n - 1)\frac{\pi}{4}\right), n = 1,2,3,4. \quad (13)$$

Where E_s = Energy-per-symbol and T_s =symbol duration. Therefore the signal output from the modulator is

$$[sa] = [sa_1 \ sa_2 \ sa_3 \ \dots \ sa_K] \quad (14)$$

After that, $[sa]$ enters the serial to parallel block. Then the signal output $[sb]$ will be:

$$[sb] = [sa]^T = [sa_1 \ sa_2 \ sa_3 \ \dots \ sa_N]^T \quad (15)$$

Then $[sb]$ enter the preprocessing and DMWT blocks. The transformation matrix $[W]$ will be:

$$W = \begin{bmatrix} H_0 & H_1 & H_2 & H_3 & 0 & 0 & \dots & 0 & 0 & 0 & 0 \\ 0 & 0 & H_0 & H_1 & H_2 & H_3 & \dots & 0 & 0 & 0 & 0 \\ \vdots & \vdots \\ H_2 & H_3 & 0 & 0 & 0 & 0 & \dots & 0 & 0 & H_0 & H_1 \\ G_0 & G_1 & G_2 & G_3 & 0 & 0 & \dots & 0 & 0 & 0 & 0 \\ 0 & 0 & G_0 & G_1 & G_2 & G_3 & \dots & 0 & 0 & 0 & 0 \\ \vdots & \vdots \\ 0 & 0 & 0 & 0 & 0 & 0 & \dots & G_0 & G_1 & G_2 & G_3 \\ G_2 & G_3 & 0 & 0 & 0 & 0 & \dots & 0 & 0 & G_0 & G_1 \end{bmatrix} \quad (16)$$

Fast DMWT computation for 1-D signal using critically sampling is computed using the following procedure:

- Checking input dimensions: Input vector $[sb]$ should be of length N , where N is a power of two.
- For any odd row
New odd row = (0.373615) [same odd row] + (0.11086198) [next even row] + (0.11086198) [previous even row]
- For any even row
New even row = $(\sqrt{2}-1)$ [same even row]
- Constructing an $N/2 \times N/2$ transformation matrix $[W]$ using GHM (LPF and HPF) matrices respectively. After substituting GHM matrix filter coefficients values, an $N \times N$ transformation matrix W results
- Transformation of input vector, which can be done by applying matrix multiplication between $[W]$ and $N \times 1$ vector $[sb]$. The output can be shown as:

$$[Sc] = [W] \times [sb]^T \quad (17)$$

The waveforms of the GHM Multiwavelet for the first decomposition $D = 1$ has $r = 2$. Giving to Multiwavelet system a given bandwidth can be splits into $r \times 2^D$ orthogonal subbands with a decomposition level D . therefore

$$Sc = \frac{1}{\sqrt{2^D r}} \sum_{d=0}^{2^D-1} \sum_{i=1}^r sb_{d,i} \Phi_{d,i} \quad (18)$$

$$[Sc] = DMWT[sb] = [Sc_0 Sc_1 Sc_2 \dots Sc_{N-1}] \quad (19)$$

Where the $n_{d,i}$ is the samples according to identified decomposition level D while $\Phi_{d,i}$ denotes the mother scaling function at this level.

After that the signal inputs to the subcarrier mapping block as shown in Fig. 3.

- For IFDMA, the Multiwavelet samples after subcarrier mapping $\{\widetilde{Sc}_l\}$ can be written as:

$$\widetilde{Sc}_l = \begin{cases} Sc_{l/Q} & , l = Q \cdot k \ (0 \leq k \leq N - 1) \\ 0 & , \textit{otherwise} \end{cases} \quad (20)$$

Where $0 \leq l \leq M - 1$ and $M = Q \cdot N$

Q is the bandwidth expansion factor.

- For LFDMA, the Multiwavelet samples after subcarrier mapping $\{\widetilde{Sc}_l\}$ can be written as:

$$\widetilde{Sc}_l = \begin{cases} Sc_l, & 0 \leq l \leq N - 1 \\ 0, & N \leq l \leq M - 1 \end{cases} \quad (21)$$

- For DFDMA, the Multiwavelet samples after subcarrier mapping \widetilde{Sc}_l can be written as:

$$\widetilde{Sc}_l = \begin{cases} Sc_{l/\tilde{Q}}, & l = \tilde{Q} \cdot k \ (0 \leq k \leq N - 1) \\ 0 & , \textit{otherwise} \end{cases} \text{ Where } 1 \leq \tilde{Q} \leq Q. \quad (22)$$

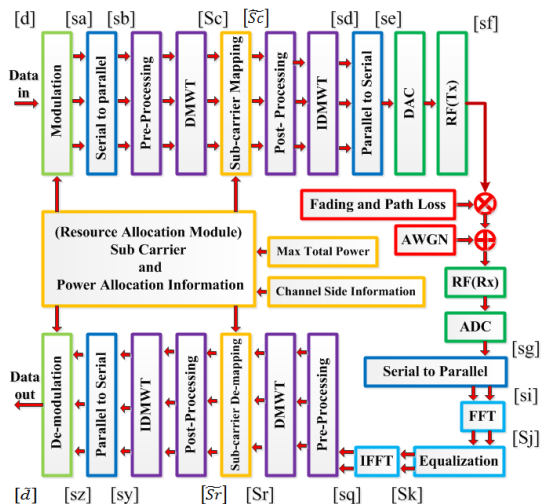


Figure 2: The block diagram of proposed DMWT-4G-LTE-SCFDMA.

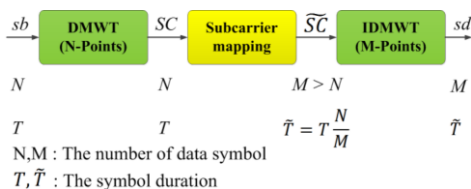


Figure 3: The process of subcarrier mapping.

Therefore the signal of samples after subcarrier mapping process is:

$$[\tilde{S}\tilde{C}] = [\tilde{S}c_0 \ \tilde{S}c_1 \ \tilde{S}c_2 \ \dots \ \tilde{S}c_{M-1}] \quad (23)$$

After the sample data output from subcarrier mapping $[\tilde{S}\tilde{C}]$ then inputs to the blocks of post processing and inverse discrete Multiwavelet transform IDMWT. In which the matrix W will be $M \times M$. this process can be summarized as:

- Let $[\tilde{S}\tilde{C}]$ is the $M \times 1$ Multiwavelet transformed vector, where M is power of 2.
- Construct $M \times M$ reconstruction matrix W_2
- Multiply a $M \times M$ reconstruction matrix W_2 with the transposed of $M \times 1$ Multiwavelet transformed vector $W_2 \times \tilde{S}\tilde{C}^T$.
- For odd row:
 Odd row = {[same odd row] - (0.11086198) [next even row] - (0.11086198) [previous even row]} / (0.373615)
- For even row
 Even row = [same even row] / $(\sqrt{2} - 1)$

Reconstructed of input transformation vector can be done as follows

$$[sd] = IDMWT[\tilde{S}c] = [W_2] \times [\tilde{S}c]^T \quad (24)$$

$$[sd] = [sd_0 \quad sd_1 \quad sd_2 \quad \dots \quad sd_{M-1}] \quad (25)$$

After that the samples input to parallel to serial convertor and the output $[se]$ will be:

$$[se] = [sd]^T = [se_0 \quad se_1 \quad se_2 \quad \dots \quad se_{M-1}] \quad (26)$$

Then the signal input to digital to analog convertor and then to radio frequency transmitter. The transmitter also does a direct filtering operation mentioned as pulse shaping to decrease out-of band signal energy. The frequency domain and time domain representations of the filter are as follows.

$$P(f) = \begin{cases} T & 0 \leq |f| \leq \frac{1-\alpha}{2T} \\ T/2 \left\{ 1 + \cos \left[\frac{\pi T}{\alpha} \left(|f| - \frac{1-\alpha}{2T} \right) \right] \right\} & \frac{1-\alpha}{2T} \leq |f| \leq \frac{1+\alpha}{2T} \\ 0 & |f| \geq \frac{1+\alpha}{2T} \end{cases} \quad (27)$$

$$P(t) = \frac{\sin(\pi t/T)}{\pi t/T} \times \frac{\cos(\alpha \pi t/T)}{1-4\alpha^2 t^2/T^2} \quad (28)$$

Where T is the symbol period and α is the roll-off factor.

Therefore the select of filter roll-off factor needs a compromise between the aims of low out-of band radiation and low PAPR.

PAPR is a performance measurement that shows the power efficiency of the source and can be defined as:

$$PAPR = \frac{\text{Peak of } se(t)}{\text{Average of } se(t)} = \frac{\max_{0 \leq t \leq MT} |se(t)|^2}{\frac{1}{MT} \int_0^{MT} |se(t)|^2 dt} \quad (29)$$

To calculate the PAPR of separate system structures, it is essential to implement the complementary cumulative distribution function (CCDF) which is the chance that PAPR is greater than a specific PAPR threshold known as PAPR0 which means $\Pr(\text{PAPR} > \text{PAPR0})$. The meaning of CCDF can be expressed as below:

$$\Pr(\text{PAPR} > \text{PAPR0}) = 1 - (1 - e^{-\text{PAPR0}})^N \quad (30)$$

Now the signal after DAC and RF blocks which is $[sf]$ travels through the channel and it suffers from two types of degradation which are noise, fading and path loss. Therefore the signal reach to the receiving end is:

$$[sg] = [h]. [sf] + n \quad (31)$$

Where $[h]$ is the impulse response of the channel and n is the noise. Then the signal enter to the serial to parallel block then the signal become

$$[si] = [sg]^T = [si_0 \ si_1 \ si_2 \ \dots \ si_{M-1}] \quad (32)$$

After that the signal $[si]$ is enters to the block of FFT and the signal become

$$[Sj] = \frac{1}{M_{FFT}} \sum_{m=0}^{M_{FFT}-1} [si] e^{-\frac{i2\pi m}{M_{FFT}}} \quad (33)$$

After that the signal enters to the block of frequency domain linear equalization. In order to describe the procedure of equalization Let $E(m)$ be the equalization coefficients, as shown in Fig. 4, where $(m=0, 1, 2, \dots, M_{FFT}-1)$ In minimum mean square error MMSE manner the equalizer coefficient is:

$$E(m) = H^*(m) / [|H(m)|^2 + (E_b/N_0)^{-1}] \quad (34)$$

Where $*$ denotes the complex conjugate, $H(n)$ describe the transfer function of the wireless channel and E_b/N_0 is average energy-per-bit to noise power spectral density. The signal after multiply the equalization parameter $E(m)$ with the FFT signal $[Sj]$ will be:

$$[Sk] = E(m) \cdot [Sj] = [Sk_0 \ Sk_1 \ Sk_2 \ \dots \ Sk_{M-1}] \quad (35)$$

The time domain equalized signal after applying IFFT which is $[sq]$ can be expressed as:

$$[sq] = \frac{1}{M_{FFT}} \sum_{m=0}^{M_{FFT}-1} [Sk] e^{\frac{i2\pi m}{M_{FFT}}} \quad (36)$$



Figure 4: The process of channel equalization

Now, the signal is enter to the blocks of preprocessing and the DMWT and the output signal is:

$$[Sr] = DMWT[sq] \quad (37)$$

Then this signal enters to subcarrier de-mapping. The output from the subcarrier de-mapping is:

$$[\tilde{Sr}] = demapping[Sr] \quad (38)$$

Then the signal enters to the blocks of post processing and IDMWT. The output signal from this block is

$$[sy] = IDMWT[\widehat{sr}] \quad (39)$$

Then the signal enter to the parallel to serial form and the output will be

$$[sz] = [sy]^T = [sy_0 \ sy_1 \ sy_2 \ \dots \ sy_{N-1}]^T \quad (40)$$

Finally, the signal $[sz]$ enters to the final block which is the demodulation. The data output is

$$[\vec{d}] = demodulation [sz] = [d_0 \ d_1 \ d_2 \ \dots \ d_K] \quad (41)$$

Results and Discussion

In this paper the proposed system of SCFDMA in 4G-LTE is implemented and tested using the MWT and FFT under the LTE channel cases which are Extended Pedestrian - A (EPA), Extended Vehicular - A (EVA) and Extended Typical Urban (ETU). The factors of the model are listed in Table I.

As shown in Fig. 5, when use the FFT the SNR is varies from 7.8 dB to 11 dB in interleaved mode and varies from 11.9 dB to 13.7 dB in localized mode. When develop the system by using the MWT, as shown in Fig. 6, the SNR will be decreased and varies from 2.9 dB to 4.9 dB at interleaved mode and from 5.5 dB to 6.9 dB at localized mode. (*This means the system based on MWT gives lower BER than system based on FFT and interleaved mode is better than localized mode*)

Now, the parameter that will be discus is the peak to average power ratio PAPR. In this parameter the relation is calculates between PAPR0 and CCDF (PAPR0). In this design three sub-parameters will be change that will effect on the values of the PAPR which are roll off factor (α), modulation types and subcarrier mapping selection. In the first parameter which is Alfa (α). Its values will be changed from 0.0 to 1.0. According to the changing of Alfa the value of PAPR0 will also change. It is notice from Fig. 7 that the value of PAPR0 will be varies from 3.4 dB to 9.5 dB when used the FFT while changed from 1.5 dB to 6.8 dB when used the MWT as shown in Fig. 8. That means the value of PAPR0 are 3.4 dB, 4.7 dB, 5.9 dB, 6.4 dB, 8 dB and 9.5 dB with α equal to 1.0, 0.8, 0.6, 0.4, 0.2 and 0.0 respectively when use the FFT while the value of PAPR0 are 1.5 dB, 2.1 dB, 3 dB, 4 dB, 5.2 dB and 6.8 dB with α equal to 1.0, 0.8, 0.6, 0.4, 0.2 and 0.0 respectively with the use of MWT. (*This means when a decreased from one to zero then the PAPR0 will be increased*).

The second parameter that is used in simulation is the types of modulation (QPSK, 16QAM and 64QAM). It can be shown from Fig. 9 that the PAPR0 is changed from 3.4 dB to 6.4 dB when apply FFT and from 1.5 dB to 3.9 dB with the use of MWT as shown in Fig. 10. This means that the values of PAPR0 are 3.4 dB, 5.3 dB and 6.6 dB with modulation of QPSK, 16QAM and 64QAM respectively with FFT while the values of PAPR0 are 1.5 dB, 2.9 dB and 3.8 dB with modulation of QPSK, 16QAM and 64QAM respectively when used the

MWT. (It can say that when the modulation type is high [such as 64QAM] then the PAPR0 is high).

The final parameter that discuss is the subcarrier mapping (Localized, Distributed and Interleaved). Now when change the subcarrier mapping the PAPR0 also change from 3.4 dB to 8.5 dB when using FFT as shown from Fig. 11 and from 1.5 dB to 5.8 dB with the use of MWT as shown in Fig. 12. This means that the values of PAPR0 is 3.4 dB, 5.3 dB and 8.5 dB for interleaved, distributed and localized respectively when using the FFT while the values of PAPR0 is 1.5 dB, 3.1 dB and 5.8 dB for interleaved, distributed and localized respectively when using the MWT. (This means the interleaved mode gives lower PAPR and localized mode gives higher PAPR while distributed mode locates in the middle).

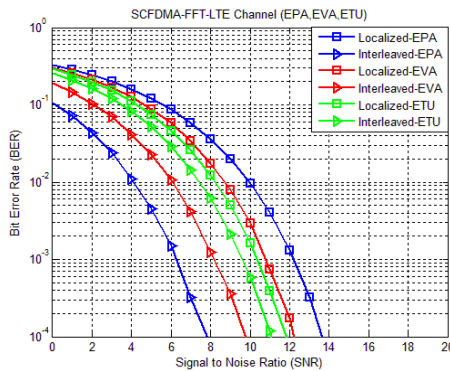


Figure 5: the LTE-SCFDMA system in FFT under different channels

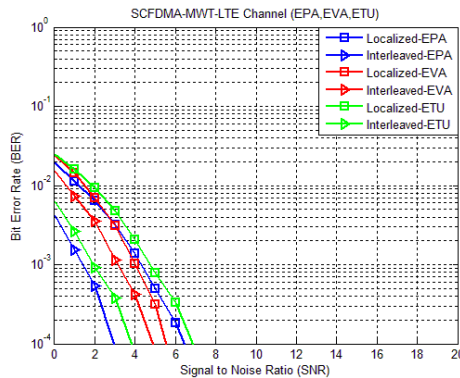


Figure 6: the LTE-SCFDMA system in MWT under different channels

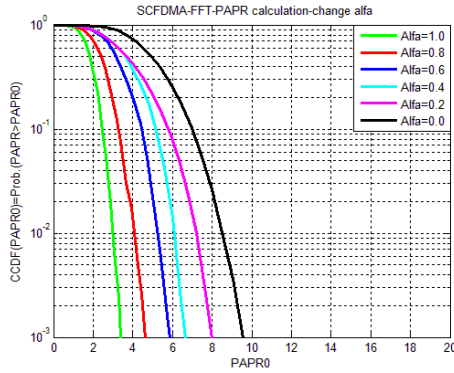


Figure 7: the LTE-SCFDMA system in FFT with multi values of α

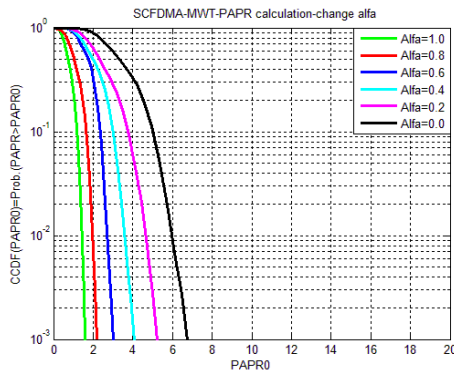


Figure 8: the LTE-SCFDMA system in MWT with multi values of α

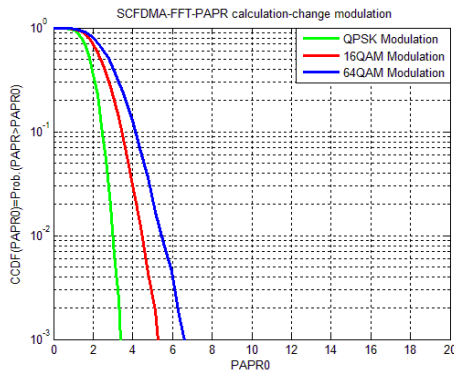


Figure 9: the LTE-SCFDMA system in FFT with different modulation

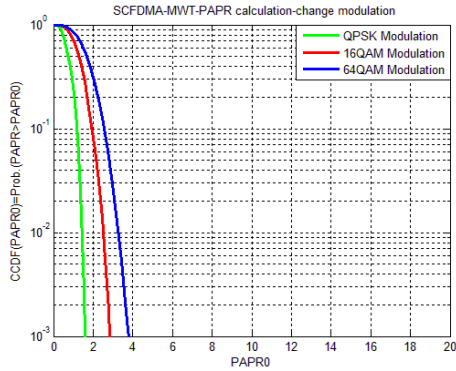


Figure 10: the LTE-SCFDMA system in MWT with different modulation

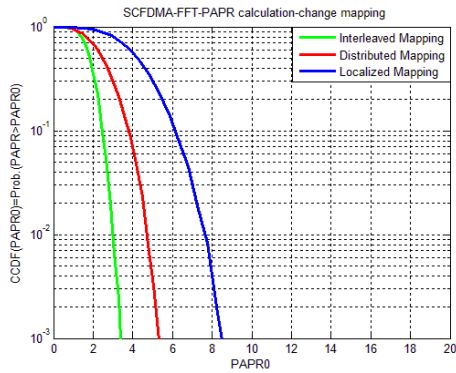


Figure 11: the LTE-SCFDMA system in FFT with different mapping

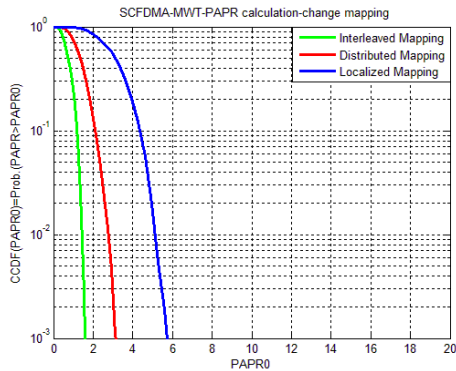


Figure 12: the LTE-SCFDMA system in MWT with different mapping

Conclusion

From all simulations and cases it can conclude that the interleaved subcarrier mode gives lower BER than localized mode in case of FFT and MWT. And the MWT gives improved performance than the FFT in case of BER tests. In case of PAPR tests it can indicate that when roll off factor increase from zero to one this lead to decrease the PAPR. When the modulation is change from QPSK to 16QAM or 64QAM then the PAPR will be bigger. It can announce that the interleaved mode gives lower PAPR than distributed and localized mode. From all tests of BER and PAPR one important fact can be shown which is: *(the MWT gives lower BER and PAPR for all cases in simulation. that means the proposed system is better than system based on the FFT)*. In the end, there is no cyclic prefix piece in transmitter and receiver system. Therefore, the proposed system is more bandwidth efficient. Thus huge data rate transmission is potential without extra bandwidth, that means the quality and magnitude of the signal spread to user will be developed.

Table 1: the parameters for 4G-LTE-SCFDMA

Parameters	Value
Modulation types	QPSK, 16QAM, 64QAM
Carrier Frequency f_c (MHz)	2400
Channel types	LTE (EPA, EVA, ETU)
Equalization type	MMSE
No. of useful carrier (N)	64
No. of total carrier (M)	1024
Target BER	10^{-4}
Target of CCDF(PAPR0)	10^{-3}
roll-off factor (α)	0.0, 0.1, 0.2, 0.4, 0.6, 0.8, 1.0
Sub carrier mapping	Localized, Distributed, Interleaved

REFERENCES

- [1] X. Fan, Li. Yuanjie, Li Mingqi, and X. Zhang, "Analysis and Comparison of Different SC-FDMA Schemes for 3GPP LTE", IEEE International Conference on Wireless Communications, Networking and Mobile Computing, WiCom07, pp. 787–790, 2007.
- [2] H. Gillian, N. Andrew, and A. Simon, "Impact of Radio Resource Allocation and Pulse Shaping on PAPR of SC-FDMA Signals", IEEE 18th International Symposium on Personal, Indoor and Mobile Radio Communications, PIMRC07, pp. 1 – 5, 2007.
- [3] G. Berardinelli, L. A. Ruiz, S. Frattasi, M. I. Rahman, and P. Mogensen, "OFDMA vs. SC-FDMA: Performance Comparison in Local Area IMT-A Scenario", IEEE Wireless communications, vol. 15, Issue 5, pp. 64 – 72, 2008.

- [4] Z. Pooneh and V. Serdean, "A Hierarchical Multiwavelet Based Stereo Correspondence Matching Technique", 19th European signal processing conference (EUSIPCO11), Barcelona, Spain, 2011.
- [5] S. M. Salih, "BER Reduction for DMT-ADSL Based on DMWT", Cankaya University Journal of Science and Engineering, ISSN 1309 – 6788, vol. 8, No. 2, pp. 237-254, , 2011.
- [6] S. Vasily, H. Peter Niels, S. Gilbert, and T. Pankaj, "The Application of Multiwavelet Filter banks to Image Processing", IEEE Transactions on Image Processing, Vol. 8, No. 4, pp. 548 – 563, 1999.
- [7] M. R. Ahmadi, H. Adibi, and R. Saadati, "Flatlet Oblique Multiwavelet for Solving Integro-Differential Equations", Dynamics of Continuous, Discrete and Impulsive Systems Series A: Mathematical Analysis, Watam Press, vol. 15 , pp. 755-768, 2008.
- [8] K. Fritz, Wavelets and Multiwavelets, CHAPMAN & HALL CRC Press Company, ISBN 1-58488-304-9, 2004.
- [9] M. Baro and I. Jacek, "Multi-band wavelet based spectrum agile Communications for Cognitive radio secondary user Communications", IEEE International Symposium on broadband multimedia systems and broadcasting, pp. 1-5, 2008.
- [10]H. Kattoush, W. A. Mahmoud, A. Mashagbah, and A. Ghodayyah, "Multiwavelet Computed Radon-Based OFDM Transceiver Designed and Simulation under Different Channel Conditions", Journal of Information and Computing Science, World Academic Press, ISSN 1746-7659, vol. 5, No. 2, , pp. 133-145, England, UK, 2010.
- [11]T. Jo Yew, S. Lixin, and T. Hwee Huat, "A General Approach for Analysis and Application of Discrete Multiwavelet Transforms", IEEE Transactions On Signal Processing, Vol. 48, No. 2, pp. 457 – 464,2000.